The QCD moat regime and its real-time properties

Wei-jie Fu [1] Jan M. Pawlowski [2,3] Robert D. Pisarski [4] Fabian Rennecke [5,6] Rui Wen [7] and Shi Yin [5,*]

arXiv:2412.15949

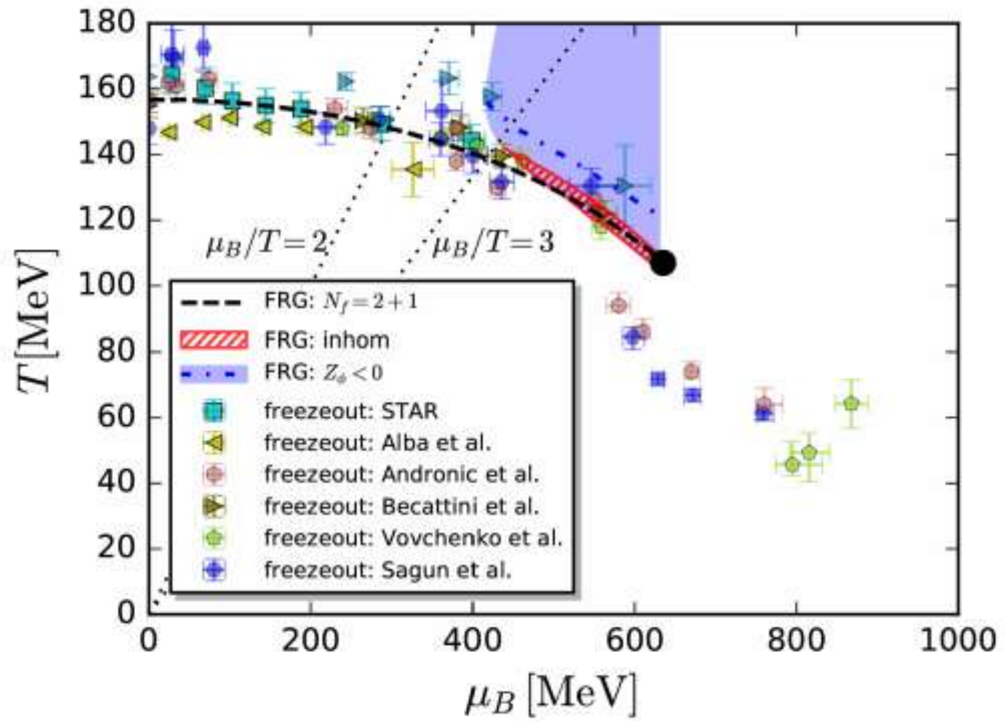

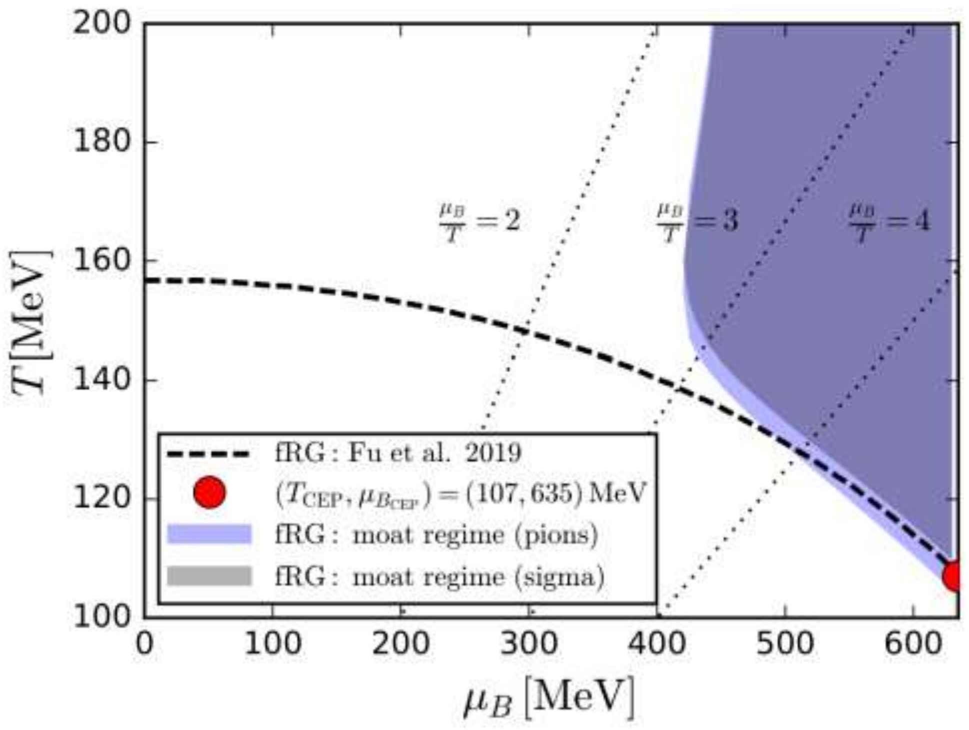

arXiv:1909.02991

The QCD moat regime and its real-time properties

Wei-jie Fu,[1] Jan M. Pawlowski,[2,3] Robert D. Pisarski,[4] Fabian Rennecke,[5,6] Rui Wen,[7] and Shi Yin[5,*]

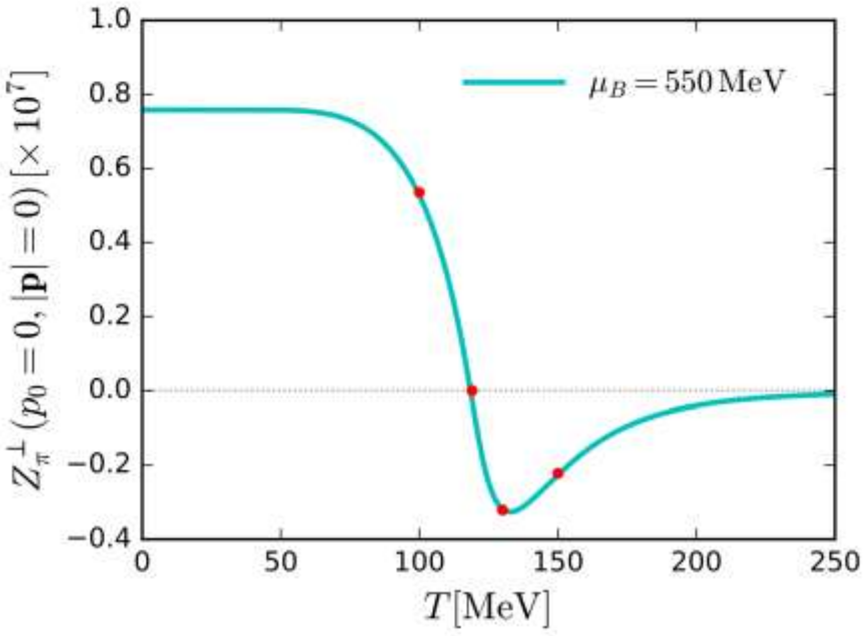

FIG. 4. Spatial pion wave functions $Z_\pi^\perp(p_0 = 0, |\boldsymbol{p}| = 0)$ as a function of temperature T, at baryon chemical potential $\mu_B = 550$ MeV. Red dots correspond to the temperatures in Fig. 10.

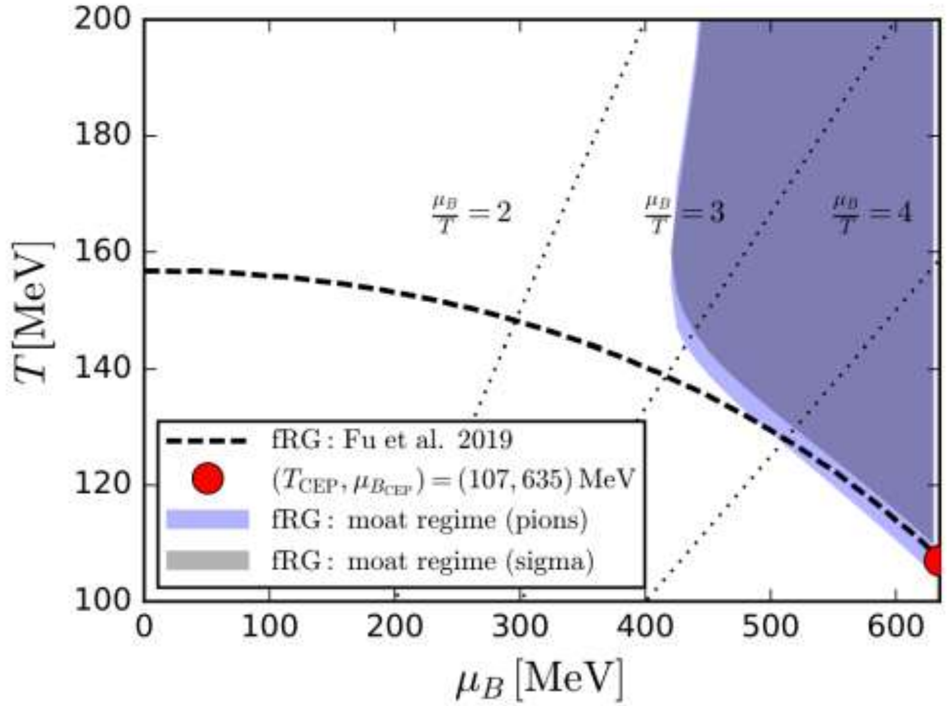

The meson propagator

$$G_\phi(p) = \langle \phi(p)\phi(-p)\rangle_c$$

$$G_\phi(p) = \frac{1}{Z_\phi^{\parallel}(p_0,\boldsymbol{p})\,\left(p_0^2 + m_\phi^2\right) + Z_\phi^{\perp}(p_0,\boldsymbol{p})\,\boldsymbol{p}^2}$$

The temporal and spatial wave functions,

Consider the static propagator $G_\phi(p)|_{p_0=0}$

$$Z_\phi^{\parallel/\perp}(\boldsymbol{p}^2) \approx Z_0^{\parallel/\perp} + Z_1^{\parallel/\perp}\boldsymbol{p}^2$$

Solve $(G_\phi^{-1})'(\boldsymbol{p}_M^2) = 0$

$$\boldsymbol{p}_M^2 = -\frac{Z_0^{\perp}}{2Z_1^{\perp}} - \frac{Z_1^{\parallel} m_\phi^2}{2Z_1^{\perp}}$$

$$G_\phi(p) \approx \frac{1}{\left(Z_0^{\parallel} + Z_1^{\parallel}\boldsymbol{p}^2\right)p_0^2 + Z_1^{\perp}\left(\boldsymbol{p}^2 - \boldsymbol{p}_M^2\right)^2 + m_{\text{eff}}^2}$$

$$m_{\text{eff}}^2 = Z_0^{\parallel} m_\phi^2 - Z_1^{\perp}\boldsymbol{p}_M^4$$

the static meson dispersion

$$E_\phi^{(\text{stat})}(\boldsymbol{p}) \equiv \sqrt{G_\phi^{-1}(\boldsymbol{p})} = \sqrt{Z_1^{\perp}\left(\boldsymbol{p}^2 - \boldsymbol{p}_M^2\right)^2 + m_{\text{eff}}^2}\,.$$

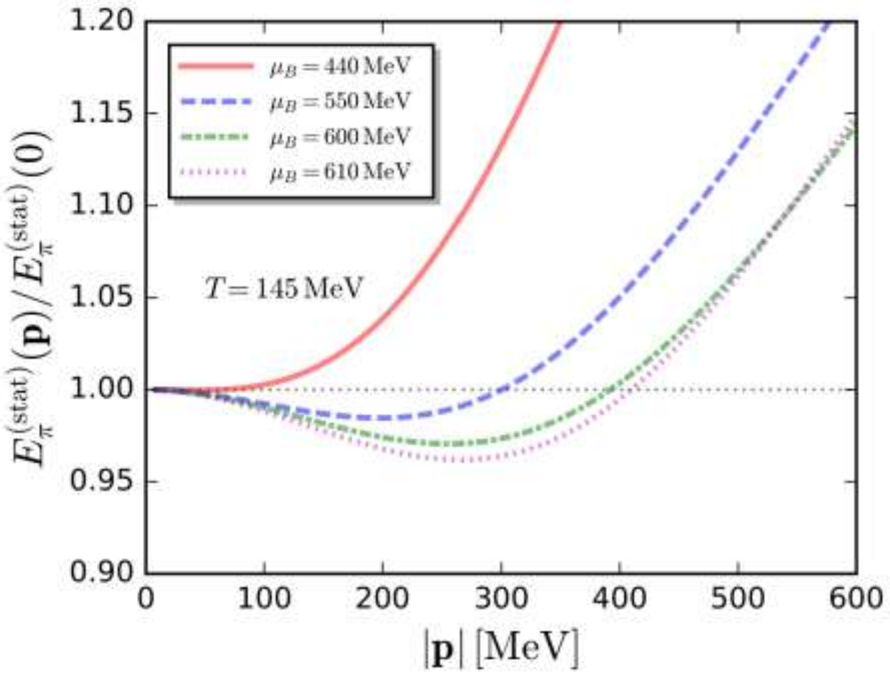

FIG. 2. Normalized static dispersion relation, defined in Eq. (8), for pions at $T = 145$ MeV and different μ_B.

the static dispersion is minimal at p = p_M

$$E_\phi^{(\text{stat})}(\boldsymbol{p}_M) = m_{\text{eff}} \le m_\phi\,.$$

if $Z_1^{\perp}\boldsymbol{p}_M^4 \ge m_\phi^2$ energy gap vanishes or even turns imaginary

inhomogeneous instabilities in QCD

QCD spectral functions from the functional renormalisation group

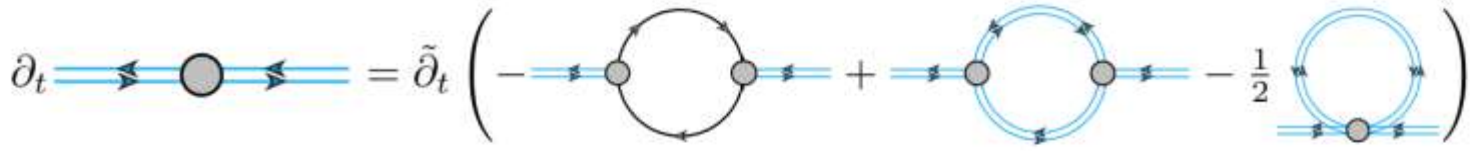

$$p_0 \to -\mathrm{i}(\omega \pm \mathrm{i}\epsilon)$$

$$\rho_\phi(\omega, \boldsymbol{p}) = \frac{1}{\pi} \mathrm{Im}\, G_\phi^R(\omega, \boldsymbol{p})\,.$$

$$G_\phi^R(\omega, \boldsymbol{p}) = \lim_{\epsilon \to 0^+} G_\phi\big(-\mathrm{i}(\omega + \mathrm{i}\epsilon), \boldsymbol{p}\big)$$

In practice, we do this in a two-step procedure.

1.We solve the fully coupled QCD system without taking into account the full momentum dependence of the propagators, cf. Ref. [3]

2.We then use these results as input to separately solve the flow equation of the fully momentum dependent two-point functions shown in Fig. 3

QCD spectral functions from the functional renormalisation group

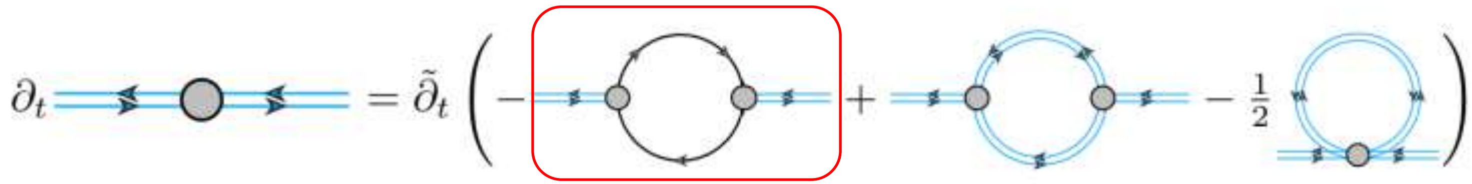

$$\tilde{\partial}_t (\Pi^{\phi\phi}_{\mathrm{QL}})_{ij}(p) = -2N_c \frac{h_k^2}{k\, Z_{q,k}^2}\delta_{ij} \int \frac{d^3\boldsymbol{q}}{(2\pi)^3}\Big[1 + (|\boldsymbol{q}|/k - 1)\eta_{q,k}\Big]\Theta(1 - \boldsymbol{q}^2/k^2)$$

$$\times \Bigg\{ -2\mathcal{F}_{(2)} + \Big[1 + \frac{(\boldsymbol{q}-\boldsymbol{p})^2}{k^2}(1 + r_q((\boldsymbol{q}-\boldsymbol{p})^2/k^2))^2 + \frac{p_0^2}{k^2} - 2\frac{\boldsymbol{q}\cdot(\boldsymbol{q}-\boldsymbol{p})}{k^2}\big(1 + r_q(\boldsymbol{q}^2/k^2)\big)\big(1 + r_q((\boldsymbol{q}-\boldsymbol{p})^2/k^2)\big)\Big]\mathcal{FF}^-_{(2,1)}$$

$$+ \Big[1 + \frac{(\boldsymbol{q}+\boldsymbol{p})^2}{k^2}(1 + r_q((\boldsymbol{q}+\boldsymbol{p})^2/k^2))^2 + \frac{p_0^2}{k^2} - 2\frac{\boldsymbol{q}\cdot(\boldsymbol{q}+\boldsymbol{p})}{k^2}\big(1 + r_q(\boldsymbol{q}^2/k^2)\big)\big(1 + r_q((\boldsymbol{q}+\boldsymbol{p})^2/k^2)\big)\Big]\mathcal{FF}^+_{(2,1)}$$

$$+ \Big[-1 + \frac{\boldsymbol{q}\cdot(\boldsymbol{q}-\boldsymbol{p})}{k^2}\big(1 + r_q(\boldsymbol{q}^2/k^2)\big)\big(1 + r_q((\boldsymbol{q}-\boldsymbol{p})^2/k^2)\big)\Big]\mathcal{FF}^-_{(1,1)}$$

$$+ \Big[-1 + \frac{\boldsymbol{q}\cdot(\boldsymbol{q}+\boldsymbol{p})}{k^2}\big(1 + r_q(\boldsymbol{q}^2/k^2)\big)\big(1 + r_q((\boldsymbol{q}+\boldsymbol{p})^2/k^2)\big)\Big]\mathcal{FF}^+_{(1,1)}\Bigg\}. \tag{B1}$$

$$\mathcal{FF}^{\pm}_{(m,n)}(p) \equiv k^{2(m+n)-1}\, T\sum_{n_q}\Big(\bar{G}_q(q,\bar{m}_q^2)\Big)^m\Big(\bar{G}_q(q\pm p,\bar{m}_q^2)\Big)^n ,$$

$$\mathcal{FF}^{\pm}_{(1,1)}(p) = \mathcal{FF}^{\pm,\mathrm{CA}}_{(1,1)}(p) + \mathcal{FF}^{\pm,\mathrm{PH}}_{(1,1)}(p) ,$$

QCD spectral functions from the functional renormalisation group

$$\mathcal{F}\mathcal{F}^{\pm,\mathrm{CA}}_{(1,1)}(p) = \frac{k^3}{4E(|\boldsymbol{q}|)E(|\boldsymbol{q}\pm\boldsymbol{p}|)}\left\{\frac{1}{ip_0 - E(|\boldsymbol{q}|) - E(|\boldsymbol{q}\pm\boldsymbol{p}|)}\Big[-1 + n_F(E(|\boldsymbol{q}|);T,\pm\mu) + n_F(E(|\boldsymbol{q}\pm\boldsymbol{p}|);T,\mp\mu)\Big] + \frac{1}{ip_0 + E(|\boldsymbol{q}|) + E(|\boldsymbol{q}\pm\boldsymbol{p}|)}\Big[1 - n_F(E(|\boldsymbol{q}|);T,\mp\mu) - n_F(E(|\boldsymbol{q}\pm\boldsymbol{p}|);T,\pm\mu)\Big]\right\},$$

$$\bar{G}_q(q) = \frac{1}{(q_0 + i\mu)^2 + \big(E(|\boldsymbol{q}|)\big)^2}$$

$$\bar{G}_q(q) = \frac{1}{(iq_0) - \big[E(|\boldsymbol{q}| - \mu)\big]} \cdot \frac{1}{(iq_0) - \big[-E(|\boldsymbol{q}| - \mu)\big]}$$

$$\mathcal{F}\mathcal{F}^{\pm,\mathrm{CA}}_{(1,1)}(p)$$

$$\frac{1}{p_0 \pm \big[E(|\boldsymbol{q}|) + E(|\boldsymbol{q}\pm\boldsymbol{p}|)\big]}$$

$$\mathcal{F}\mathcal{F}^{\pm,\mathrm{PH}}_{(1,1)}(p) = \frac{k^3}{4E(|\boldsymbol{q}|)E(|\boldsymbol{q}\pm\boldsymbol{p}|)}\left\{\frac{1}{ip_0 - E(|\boldsymbol{q}|) + E(|\boldsymbol{q}\pm\boldsymbol{p}|)}\Big[-n_F(E(|\boldsymbol{q}|);T,\mp\mu) + n_F(E(|\boldsymbol{q}\pm\boldsymbol{p}|);T,\mp\mu)\Big] + \frac{1}{ip_0 + E(|\boldsymbol{q}|) - E(|\boldsymbol{q}\pm\boldsymbol{p}|)}\Big[n_F(E(|\boldsymbol{q}|);T,\pm\mu) - n_F(E(|\boldsymbol{q}\pm\boldsymbol{p}|);T,\pm\mu)\Big]\right\},$$

$$\mathcal{F}\mathcal{F}^{\pm,\mathrm{PH}}_{(1,1)}(p) \qquad \frac{1}{p_0 \pm \big[E(|\boldsymbol{q}|) - E(|\boldsymbol{q}\pm\boldsymbol{p}|)\big]}$$

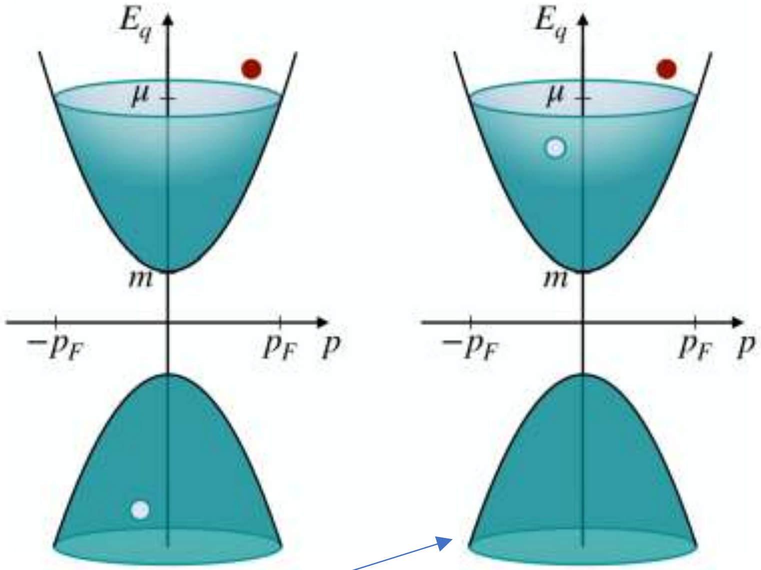

FIG. 5. Dirac cones illustrating the different quark processes contributing to the meson propagator. The Dirac cones reflect the quark dispersion $E_q(p)$. The green surface denotes the Dirac sea, which, at zero temperature, is filled up to the Fermi surface defined by $E_q(p_F) = \mu$, where p_F is the Fermi momentum. At finite T, the Fermi surface is washed out, indicated by the fading color. The red dots denote quarks and the light dots either antiquarks (left) or quark-holes (right). *Left:* Creation-annihilation (CA) process involving fluctuations of a quark-antiquark pair. This process also includes the vacuum fluctuations of quarks. *Right:* Particle-hole (PH) process involving a quark–quark-hole pair. In the non-relativistic limit, the negative energy cone vanishes and only PH processes can occur.

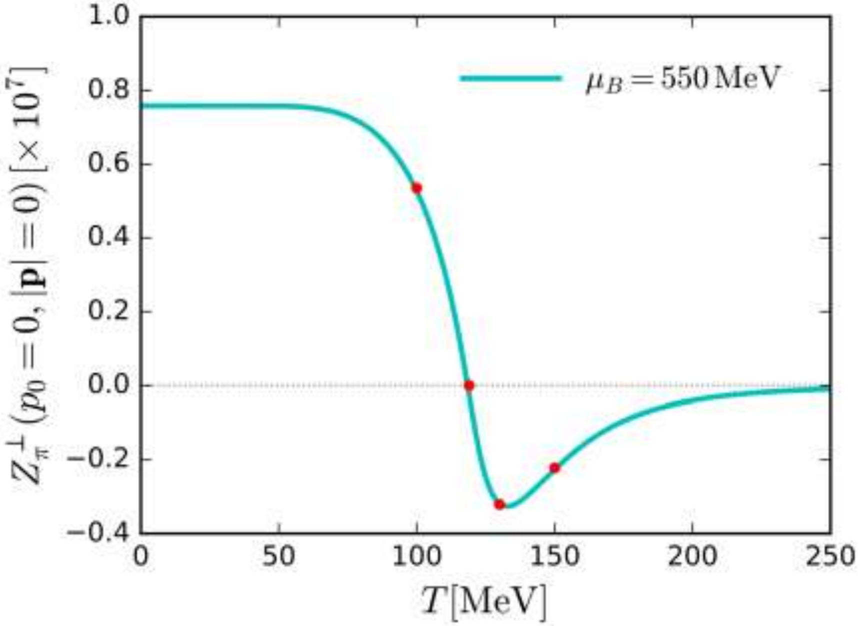

FIG. 4. Spatial pion wave functions $Z_\pi^\perp(p_0 = 0, |\boldsymbol{p}| = 0)$ as a function of temperature T, at baryon chemical potential $\mu_B = 550$ MeV. Red dots correspond to the temperatures in Fig. 10.

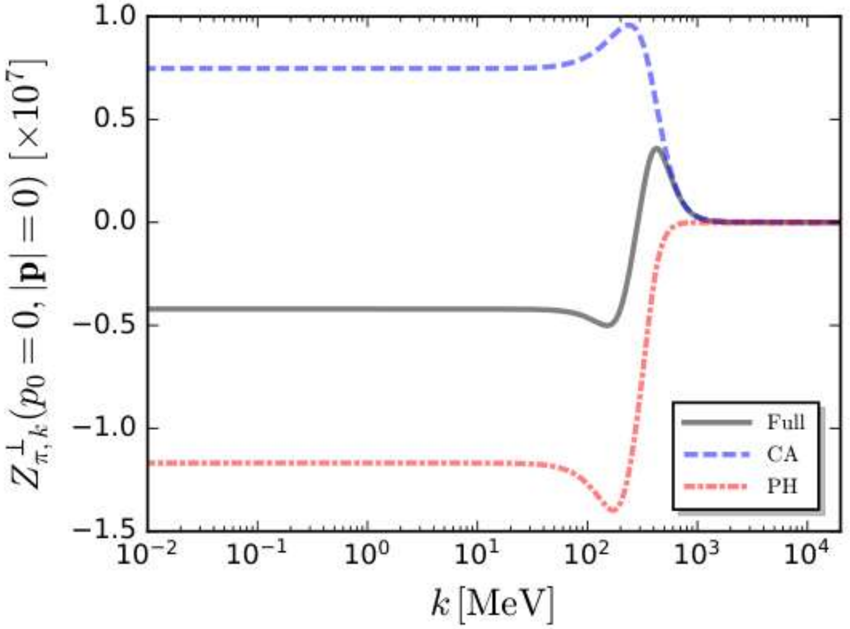

FIG. 6. Spatial pion wave function $Z_{\pi,k}^\perp(p_0 = 0, |\boldsymbol{p}| = 0)$ as a function of the RG scale k calculated at $T = 120$ MeV and $\mu_B = 600$ MeV. The solid black line shows the full re-

Real-time correlations in the moat regime

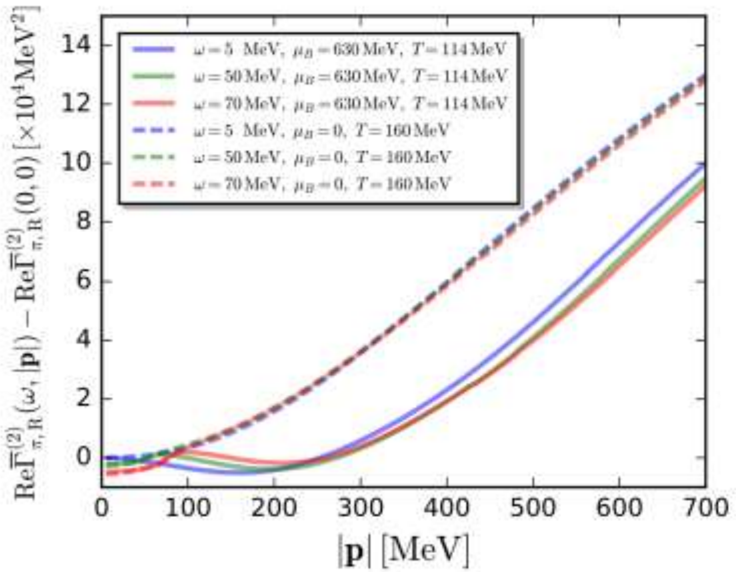

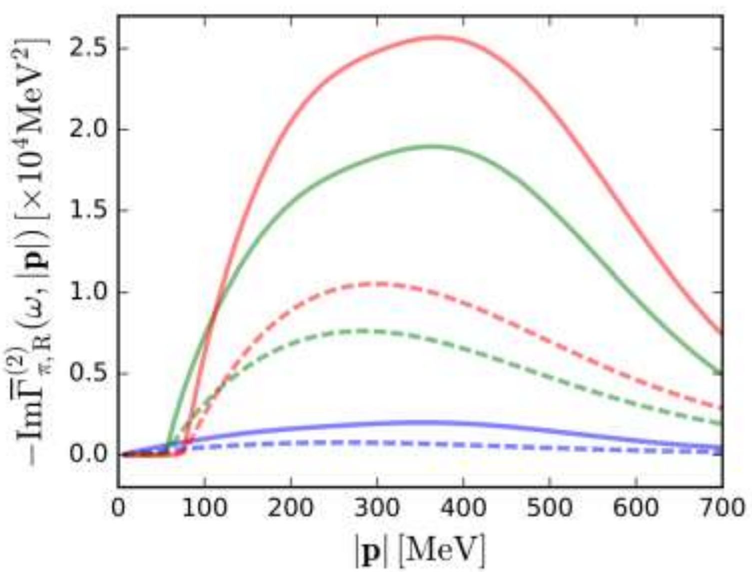

Results at large μB (solid lines) are in comparison to those at vanishing μB (dashed lines).

the moat behavior induced by PH fluctuations discussed in the previous section at ω = 0 extends to finite ω in the spacelike region of the pion two-point function.

the moat regime manifests itself most clearly in the real part of the retarded two-point function,

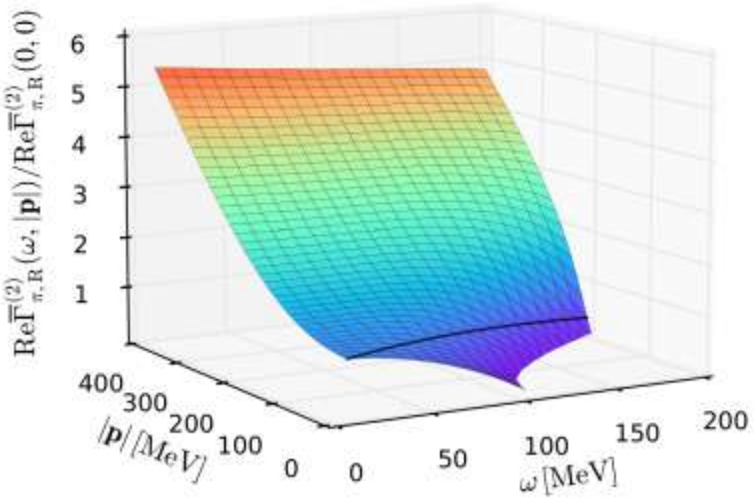

$\mu_B = 0,\ T = 160$ MeV

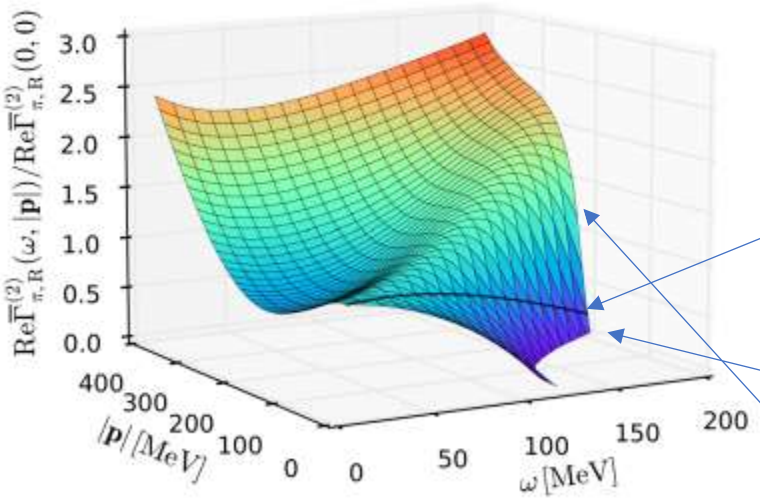

$\mu_B = 630,\ T = 114$ MeV

Light cone

$\mathrm{Re}\,\Gamma^{(2)}_{\pi,R}(\omega = E_\pi, \boldsymbol{p}) = 0$

$m_\pi^{\mathrm{pole}} = E_\pi(\mathbf{0})$

asymptotically free,

Light cone

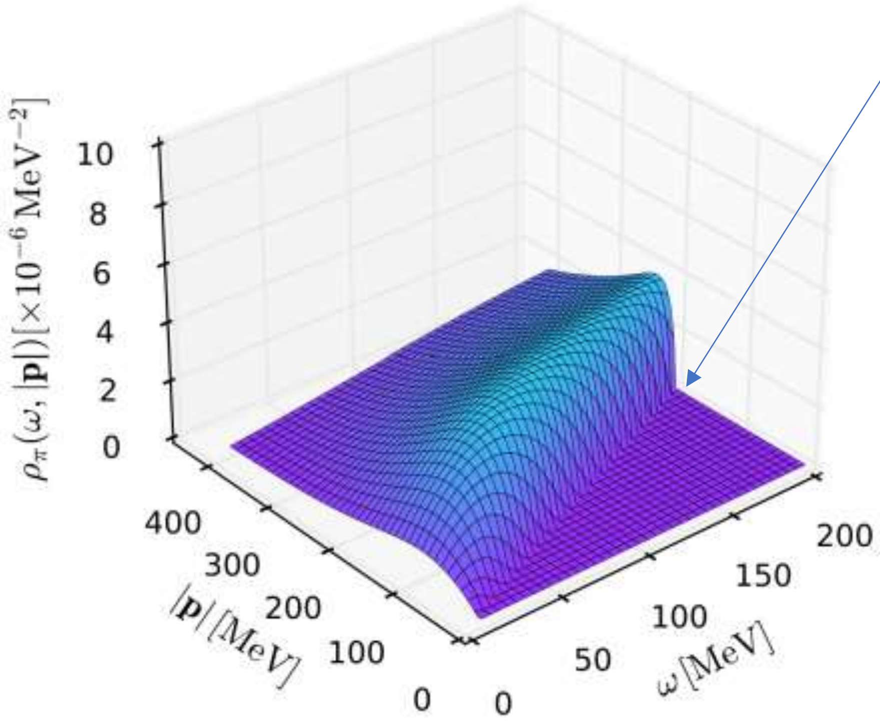

$\mu_B = 0,\, T = 160$ MeV

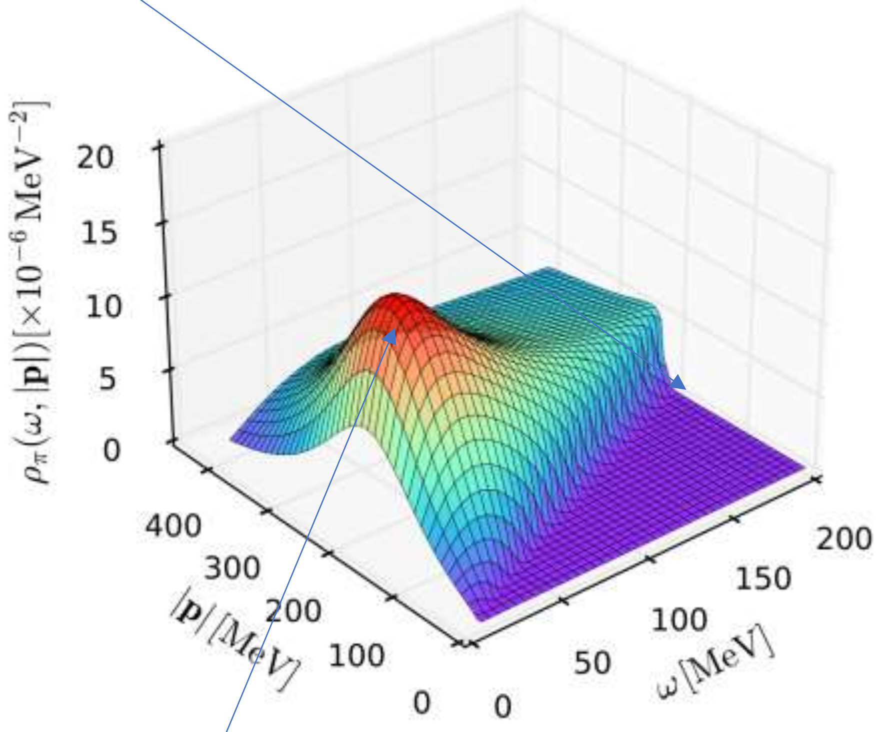

$\mu_B = 630,\, T = 114$ MeV

peak around $\omega \approx 50$ MeV and $|p| \approx 200$ MeV

This peak shows that in addition to the normal pion mode, there is another relevant contribution to the pion spectrum that may be attributed to a spacelike quasiparticle, the moaton.

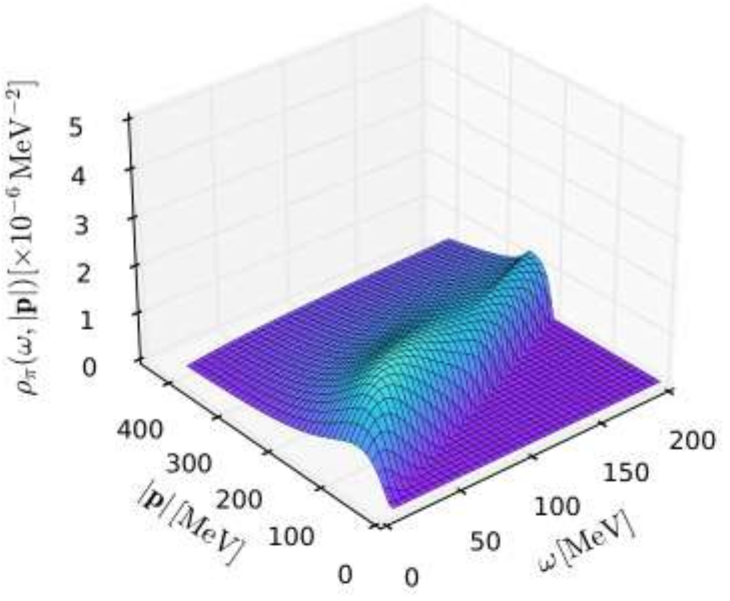

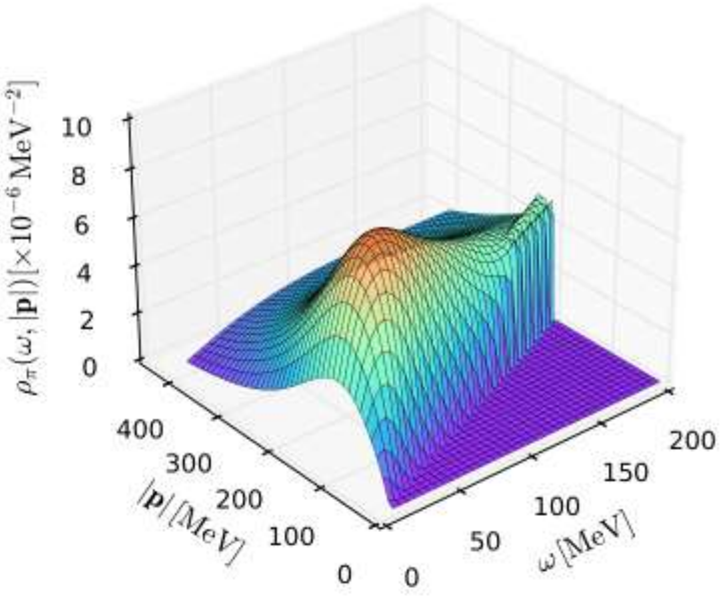

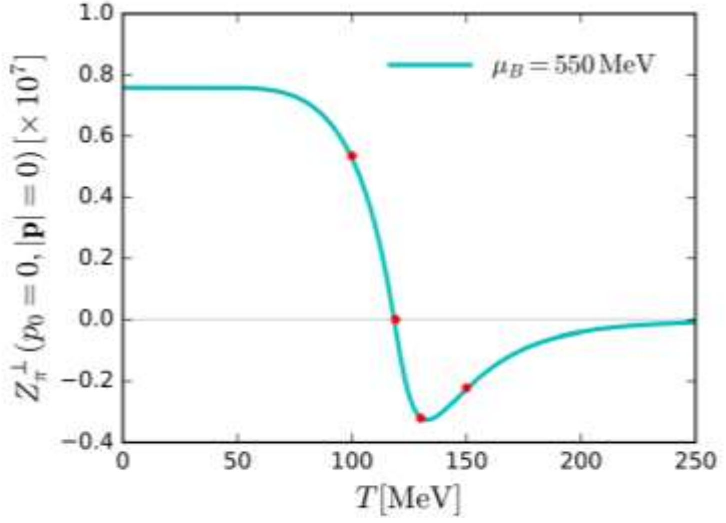

$$\mu_B = 550 \text{ MeV},$$

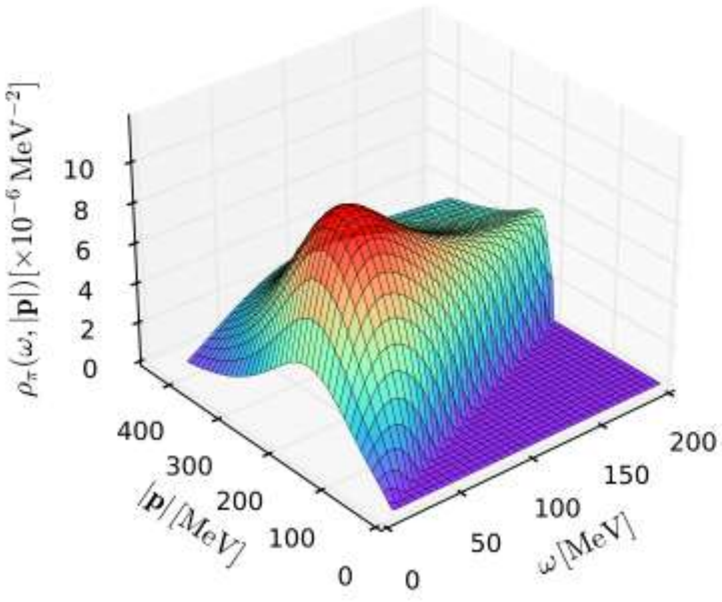

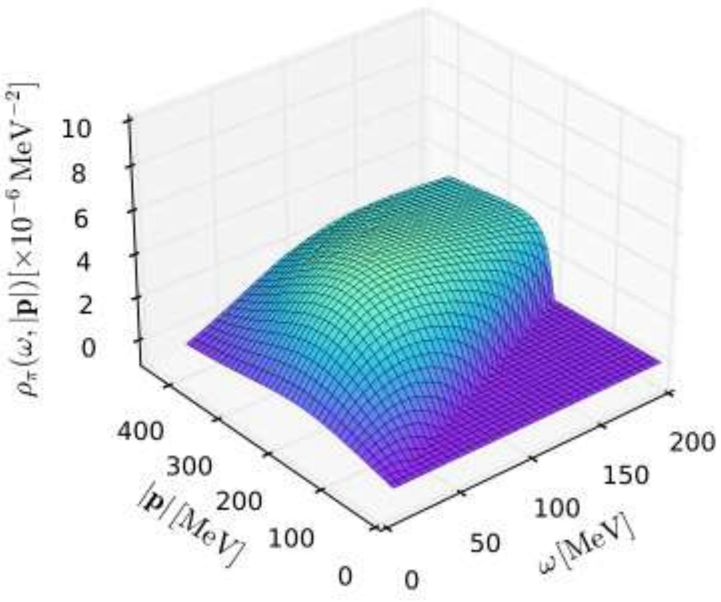

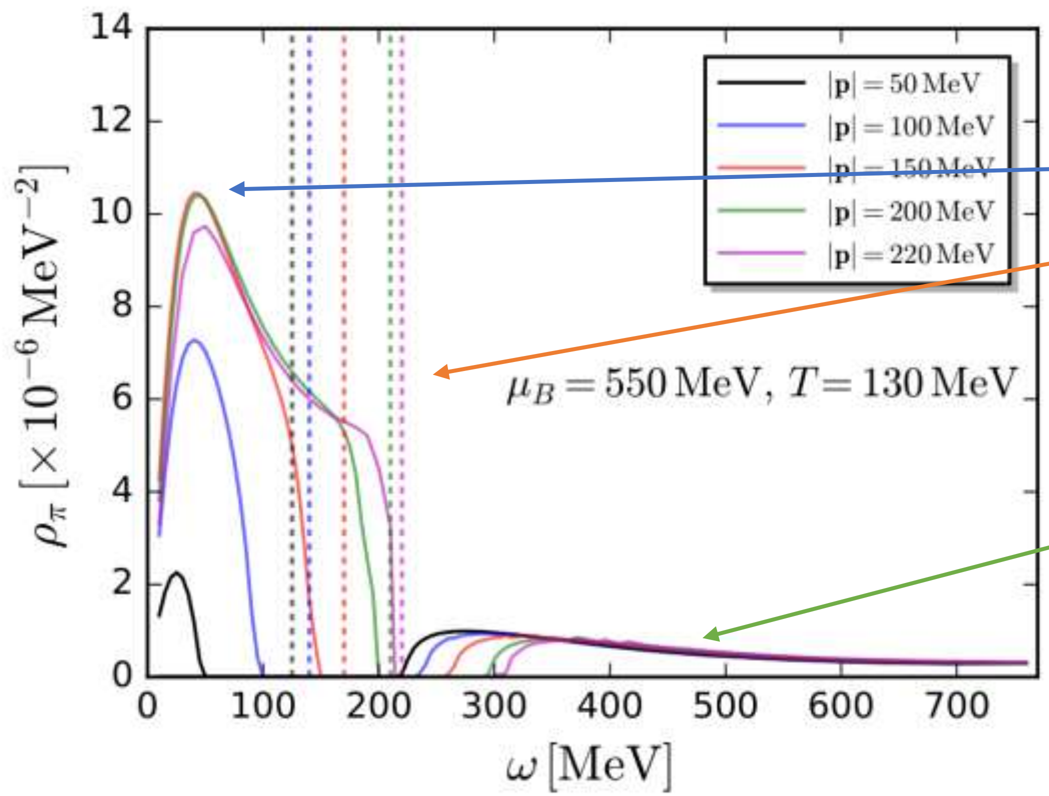

at $T = 130\,\mathrm{MeV}$ and $\mu_B = 550\,\mathrm{MeV}$. We clearly see three distinct contributions: the spacelike part from PH fluctuations, the pion particle pole (dashed line) from the zero-crossings of $\mathrm{Re}\,\Gamma^{(2)}_{\pi,R}$, and the timelike contributions dominated by the the decay of pions into quark-antiquark pairs. Most remarkably, the the moaton peak at nonzero

the timelike contribution. Since the spectral weight leads to experimental signatures from in-medium modifications [21, 61, 62], this enhancement could be the key to the experimental discovery of the moat regime.

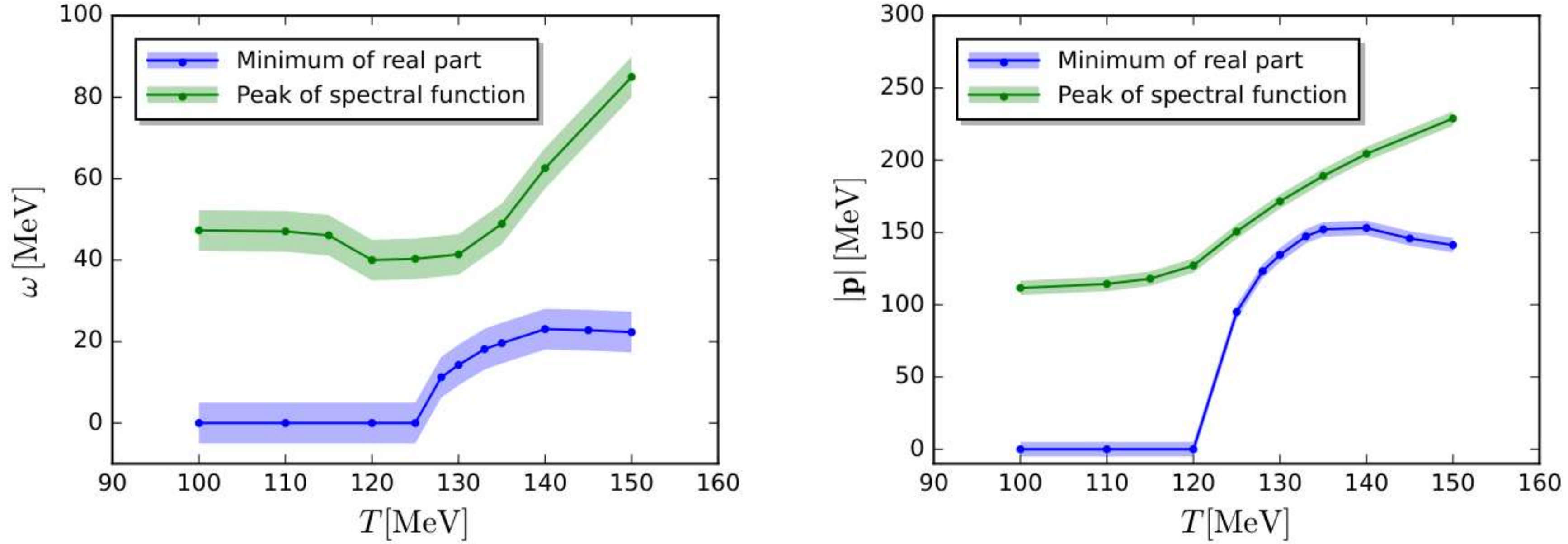

FIG. 12. The behavior of ω (left) and $|\mathbf{p}|$ (right), corresponding to the minimum in the space-like region of real part of the two-point functions (blue), and the moaton peak of spectral functions (green), as functions of temperature at $\mu_B = 550$ MeV.

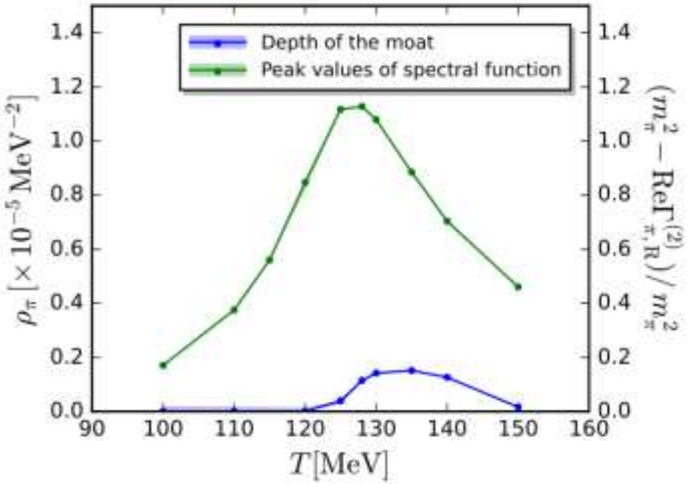

FIG. 13. Height of the moaton peak in the pion spectral function (green) and the depth of the moat (blue) as functions of T at $\mu_B = 550$ MeV. The depth of the moat is defined in Eq. (20).

In summary, we found that the pion spectral function develops a new peak in the spacelike region in the moat regime. We have shown that it can be identified as a quasiparticle, the moaton, which controls the physics of the moat regime.

Stability analysis

the static meson dispersion

$$E_\phi^{(\mathrm{stat})}(\boldsymbol{p}) \equiv \sqrt{G_\phi^{-1}(\boldsymbol{p})} = \sqrt{Z_1^\perp \left(\boldsymbol{p}^2 - \boldsymbol{p}_M^2\right)^2 + m_{\mathrm{eff}}^2}\,.$$

the static dispersion is minimal at p = p_M

$$E_\phi^{(\mathrm{stat})}(\boldsymbol{p}_M) = m_{\mathrm{eff}} \le m_\phi\,.$$

if $Z_1^\perp \boldsymbol{p}_M^4 \ge m_\phi^2$ energy gap vanishes or even turns imaginary

inhomogeneous instabilities in QCD

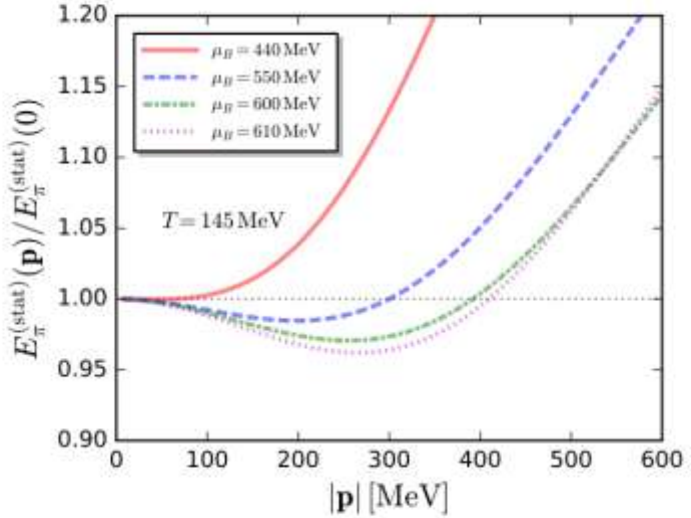

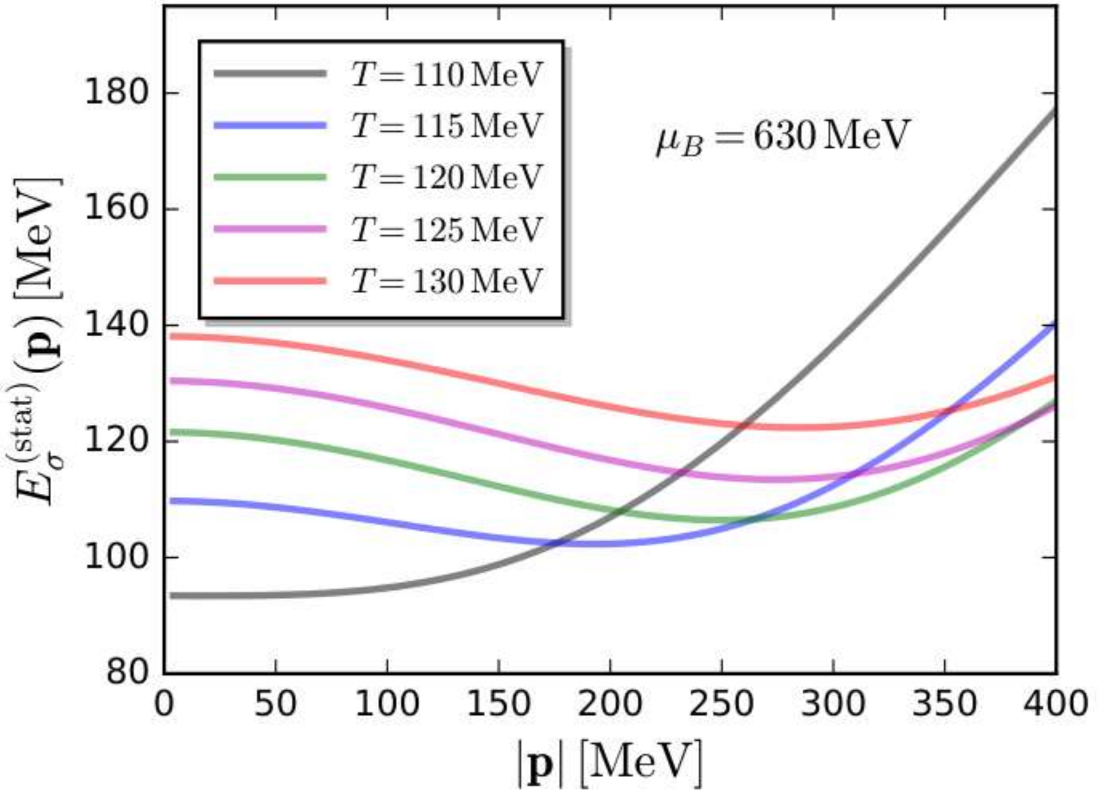

lower μ_B, so we can exclude the occurrence of an inhomogeneous instability in the QCD for all $\mu_B \le 630\,\mathrm{MeV}$.

CONCLUSION

We have shown that the moat regime arises from particlehole fluctuations of quarks at baryon chemical potentials $\mu B \gtrsim 430$ MeV above and around the pseudocritical temperature of the chiral transition. In fact, there always is a competition between creation-annihilation and particle-hole processes, where only the latter can lead to a moat regime.

The real-time properties of the moat regime have been investigated in detail through the pion spectral function. Since particle-hole fluctuations are only kinematically allowed for spacelike mesons, they exclusive contribute to the spacelike region of the spectral function. In this region, we discovered a characteristic quasiparticle-like peak in the moat regime. We have demonstrated that this peak is a manifestation of the moat regime and hence dubbed this quasiparticle moaton.